Samaras et al., Aerosol and Air Quality Research, Vol. 8, No. 1, pp. 37-53, 2008

Theoretical Investigation of the Nucleation Mode Formation Downstream of Diesel After-treatment Devices

Elias Vouitsis, Leonidas Ntziachristos, Zissis Samaras*

Laboratory of Applied Thermodynamics, Mechanical Engineering Department
Aristotle University Thessaloniki, P.O. Box 458, GR 541 24 Thessaloniki, Greece

Abstract

This study presents a modeling approach to the formation and growth of nucleation mode particles when sampling aerosol from the exhaust of a diesel engine. The simulation assumes primary particle formation due to sulphuric acid nucleation and subsequent particle growth as hydrocarbons condense on the primary nuclei. The modeling results are validated against experimental data of particle number concentrations at various dilution ratios and aging times after raw exhaust sampling. In addition, exhaust aerosol of different characteristics is produced by fitting in the engine exhaust line a diesel oxidation catalyst, a diesel particle filter, and a combination of the two. The model is able to satisfactorily reproduce the particle number and mass concentrations of exhaust particles in the nucleation mode for a variety of sampling and after-treatment conditions, with a small delay (50-200 ms) in the initiation of nucleation compared to the experiments. The measured and simulated particle concentrations are in the same order of magnitude with the exact simulated values, depending on the fuel-sulphur conversion rate and the profile of organics considered in the exhaust. This study indicates that a detailed chemical analysis of the exhaust gas, including organic speciation and sulphuric acid concentration, combined with an aerosol dynamics model, would result in a satisfactory prediction of the effect of after-treatment devices and sampling conditions on the exhaust aerosol characteristics. However, it should be stressed that modeling of diesel-exhaust processes is still in an early phase and further work is merited to better understand the processes and mechanisms involved.

Keywords: Diesel; Nanoparticles; Sampling; Dilution; Aging.

INTRODUCTION

Ambient ultrafine (< 100 nm) particles are commonly measured in a broad range of geographical locations and atmospheric conditions (e.g., Hussein *et al*., 2004, Kittelson *et al*., 2004; Zhang *et al*., 2004; 2005). In urban areas, diesel powered vehicles are primary

*Corresponding author. Tel.: +30-2310-996047, 996014, Fax: +30-2310-996019
E-*mail address*: zisis@auth.gr

emitters of such particles. New technologies, such as diesel particulate filters (DPF), may eliminate soot particles (solid fraction–accumulation mode (AM), mean diameter > 50 nm); but nanoparticles (volatile and semi-volatile fraction - nucleation mode (NM), mean diameter < 50 nm) may still be present in high numbers due to the nucleation of species after dilution and cooling of the exhaust (Abdul-Khalek *et al*., 1998; Ntziachristos *et al*., 2004a; Vaaraslahti *et al*., 2004; Burtscher, 2005; Rönkko *et al*., 2006). This is further confirmed by road chase experiments, which suggest that volatile nanoparticles are formed in the wake of the diesel vehicle during the atmospheric dilution of exhaust aerosol (Vogt *et al*., 2003; Giechaskiel *et al*., 2005; Rönkkö *et al*., 2006).

The formation of diesel NM is mainly associated with the fuel sulphur content; however, particles in this size range can be detected even at near zero fuel-sulphur levels (Vaaraslahti *et al*., 2004; Vouitsis *et al*., 2005). This implies that the contribution of the lube oil sulphur (Vaaraslahti *et al*., 2005) or other species present in the exhaust are able to give stable nuclei clusters (i.e. up to 3-5 nm) for further growth. Ammonia, for example, is such a component which may be present in high concentrations in the exhaust when low-sulphur fuel is used (CONCAWE, 2000). Other suggestions include chemiions generated during combustion (ion–induced nucleation, Yu *et al*., 2003) and particle fragmentation (Gramotnev and Gramotnev, 2005).

After nucleation, nuclei grow by coagulation and gas-to-particle conversion to form nanoparticles. The studies of Sakurai *et al*. (2003) and Tobias *et al*. (2001) suggest that organic carbon condenses on the primary nuclei, since NM particles were found to consist mainly of alkanes originating from unburned fuel and lubricating oil and a smaller fraction (up to 5% of total mass) of sulphuric acid (SA). Only at high fuel-sulphur content (360 ppm), nanoparticles were found to consist of a high sulphate fraction and a smaller amount of organic material (Scheer *et al*., 2005). Furthermore, Mathis *et al*. (2004a) studied nucleation of nanoparticles by adding different organic compounds to the dilution air and found that, depending on the functional group, hydrocarbons were capable of increasing (alcohols and toluene) or decreasing (acetone, aniline, methyl tert-butyl ether) the volume of nanoparticles.

The volatile nature of NM particles and the strong non-linear dependence of nucleation on saturation ratio introduce difficulties to the repeatable measurement of exhaust aerosol in the laboratory. The saturation ratio of condensing species depends both on the experimental conditions (dilution ratio, temperature, humidity) and on the engine/vehicle operating conditions (exhaust temperature, soot and semi-volatile species concentration) (Abdul-Khalek *et al*., 1998; Mathis *et al*., 2004b; Ntziachristos *et a*l., 2004b). Therefore, when NM particles are measured in the laboratory, one needs to distinguish between effects attributed to either the source (vehicle and fuel) or the sampling system and conditions. This is necessary in order to compare measurements from engines measured in different laboratories with different

sampling and dilution procedures, or to explain effects encountered in the lab, but not seen under atmospheric dilution conditions. In this context, modeling studies are useful in giving insight into the processes that take place and in quantifying the effect of sampling conditions on the measured aerosol properties.

In this paper we investigate the potential of NM formation and growth as engine, after-treatment and sampling conditions change, using a model to simulate gas-to-particle processes and aerosol dynamics. A series of dedicated experiments were conducted on the exhaust of a light-duty diesel vehicle by applying a well-defined sampling procedure (Ntziachristos *et al.,* 2005b). The measured results were replicated by applying the Vouitsis *et al*. (2005) model, which was extended to include the effect of the exhaust dilution and the influence from different hydrocarbon species condensation. The modeled results are then discussed in order to identify the potential of using theoretical investigations, instead of experiments, to predict the effect of after-treatment devices and sampling conditions on the exhaust aerosol characteristics, as a more cost-effective option.

METHODS

Experimental

Engine, fuel, after-treatment, and driving modes

Particle exhaust size distribution measurements were obtained from a Euro 1-compliant (1996 model VW Golf) light duty diesel engine operating in steady-state tests.

The engine was first tested with no after-treatment devices, in order to obtain exhaust samples with relatively high soot and organic semi-volatile species concentration. A diesel oxidation catalyst (DOC) was subsequently fitted in the exhaust line to reduce the concentration of organic species, without significantly affecting the soot mode. Additionally, the DOC is expected to increase sulphates by further oxidising the SO_2 emitted by the engine to SO_3. Moreover, the engine was tested with the DOC replaced by a silicon carbide diesel particle filter to reduce the soot concentration in the exhaust. DPFs have been shown to reduce solid particle number concentration by more than three orders of magnitude (e.g., Ntziachristos *et al*., 2005a).

Particle size distributions were obtained at a moderate speed of 2000 rpm and a medium (*ML* = 50%) and high load (*HL* = 90%) to obtain exhaust samples of different temperature and species concentration. The diesel fuel used fulfilled the year 2005 specifications in Europe and had a sulphur content of 50 ppm wt. The multigrade lubricating oil was used with a sulphur content of ~0.7%. The contribution of lube oil-related sulphur to the exhaust sulphur due to oil consumption can be considered negligible since its relative contribution starts to become significant for fuel-sulphur contents of 15 ppm or less (Air Resources Board, 2003).

Sampling and measurement system

Particle sampling was conducted directly from raw exhaust, employing the Fine Particle Sampler (FPS-4000) by Dekati Ltd., Tampere, Finland (Fig. 1). FPS dilutes samples in two

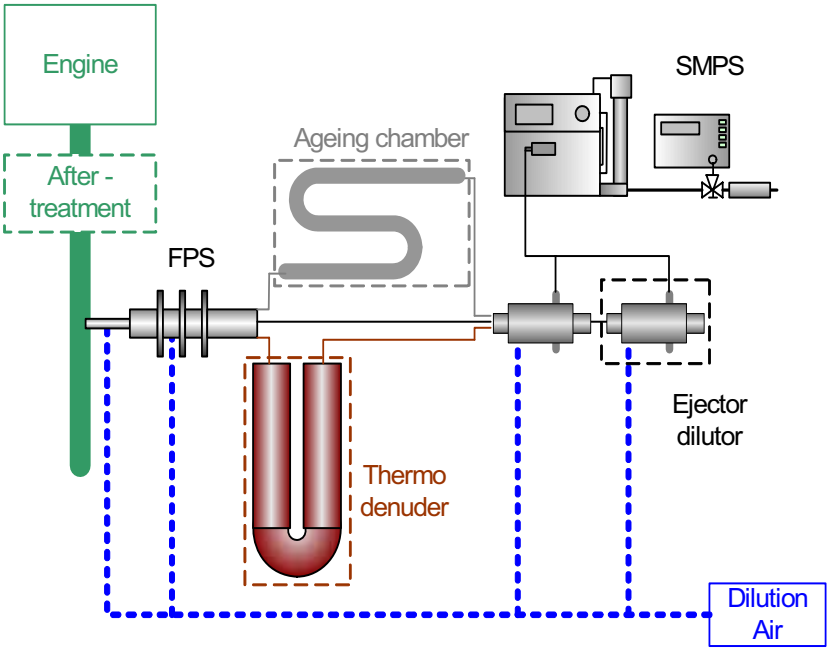

Fig. 1. Schematic of the measurement setup.

stages with purified and dry air. In the first dilution, dilution air flowing through a perforated tube gradually mixes with the exhaust sample which flows along the tube axis. This configuration eliminates particle losses and promotes nucleation. The underpressure required to draw the sample and the dilution air is produced by the second dilution stage which consists of an ejector dilutor. The dilution ratio (DR) and the dilution temperature of both stages are adjustable and controlled by altering the flowrate of the dilution air and the coolant around the dilutor respectively. This way, condensation of volatile and semi-volatile species may be maximized by keeping a low DR and a low dilution temperature, while an increase of any of these two parameters reduces condensation. More information on the operation characteristics and performance of the FPS is provided by Ntziachristos *et al.* (2005b). The DRs selected for the present tests were 10:1, 17:1, and 32:1, determined via measurement of CO_2 in the raw and the diluted exhaust. The dilution air temperature (DAT) in the porous and ejector dilution stages was set at 30°C.

A secondary dilution unit was used downstream of the FPS to quench particle formation and growth and to bring particle concentration within the range of the Scanning Mobility Particle Sizer (SMPS, model 3936L, TSI, Inc., Shoreview, MN). The SMPS size distributions have been calculated with the TSI software version that does not account for particle losses in the classifier. This may lead to some particlesinthesub-100nm range to be lost in the instrument which reduces the measured concentration of the nucleation mode. The effect of this loss is not expected to significantly affect the conclusions of this study, though, where orders of magnitude effects are sought for. The secondary dilution unit

Table 1. Time required for the completion of primary dilution in the FPS and total sample aerosol time (AT), as function of the dilution ratio.

Dilution Ratio	Completion of dilution (ms)	Short AT (ms)	Medium AT (ms)	Large AT (ms)
10:1	180	20	532	1135
17:1	100	15	406	865
32:1	55	10	265	565

consisted of two cascaded ejector diluters (DI-1000, Dekati Ltd., Tampere, Finland), each calibrated (Giechaskiel *et al*., 2004) to provide a DR of 10:1. DAT in the secondary dilution system was also kept constant at 30°C. The total DR provided by the FPS and the secondary dilution system therefore varied between 10^3:1 and 3.2×10^3:1. The dilution air used in all dilution stages was filtered by a HEPA capsule filter (Pall Corporation, East Hills, NY) and its relative humidity was reduced to less than 5% by employing a custom-made silica gel dryer. The SMPS measured particle sizes in the range between 7.6 and 290 nm, with a nominal sample flowrate of 1.0 L/min and a sheath flowrate of 10 L/min.

In order to further explore the effect of sampling conditions on the aerosol physical properties, an aging chamber of adjustable length was placed between the FPS and the secondary dilution unit to vary the aerosol aging time (AT) before analysis. Three different ATs were selected: a short, medium and long AT. The exact AT values depend on the primary DR and consequently on the total diluted sample flowrate at the FPS outlet. These values, together with the time required to complete the primary dilution in the FPS, are shown in Table 1. In some measurements, the aging chamber was replaced by a thermo-denuder (TD–ELA230, Dekati Ltd, Finland), operated at 250°C to strip soot particles from volatile and semi–volatile components.

Modeling

Vouitsis *et al.* (2005) developed an aerosol nucleation and dynamics model which was used to estimate the effect of sampling conditions on exhaust particle size distributions, with emphasis on the NM profile. The model describes aerosol aging after dilution, assuming instantaneous adiabatic dilution. The dynamics of nucleation, condensation and coagulation are then simulated for a turbulent plug flow of the sample in a cylindrical tube of diameter d and length L. The model results first showed that the measured particle number in NM can only be approached if a barrierless mechanism was assumed for the nucleation of sulphuric acid. Secondly, the total mass of NM could only be reached if hydrocarbon condensation would take place on the pre-existing sulphate nuclei. Finally, the model demonstrated the suppression of NM by the presence of soot (accumulation mode) particles, due to the competition of vapor condensation between NM and soot particles. In this study the model

is further developed by introducing the effect on particle formation of a gradual exhaust gas dilution and by including the effect of different hydrocarbons on particle growth.

When dilution is included in the modeling, the rate equations for vapor (N_i), and number (N_j) and mass (M_j) particle concentrations are given by:

Vapor molecular conc.

$$\frac{dN_i}{dt} = g_i^* J_i - \sum_{ji} R_{Cji} - R_{Wi} - \frac{1}{DR}\frac{dDR}{dt} N_i \qquad (1)$$

NM number conc.

$$\frac{dN_N}{dt} = J_i - \frac{1}{2} K_{NN} N_N^2 - K_{NA} N_N N_A - \frac{k_N}{L} N_N - \frac{1}{DR}\frac{dDR}{dt} N_N \qquad (2)$$

AM number conc.

$$\frac{dN_A}{dt} = -\frac{1}{2} K_{AA} N_A^2 - \frac{k_A}{L} N_A - \frac{1}{DR}\frac{dDR}{dt} N_A \qquad (3)$$

NM mass conc.

$$\frac{dM_N}{dt} = \sum g_i^* J_i \mu_i + \sum R_{CNi} \mu_i - K_{NA} N_N N_A \overline{M}_N - \frac{k_N}{L} M_N - \frac{1}{DR}\frac{dDR}{dt} N_N \overline{M}_N \qquad (4)$$

AM mass conc.

$$\frac{dM_A}{dt} = \sum R_{CAi} \mu_i + K_{NA} N_N N_A \overline{M}_N - \frac{k_A}{L} M_A - \frac{1}{DR}\frac{dDR}{dt} N_A \overline{M}_A \qquad (5)$$

where J_i is the nucleation rate of *i*-vapor molecules, K_{NN}, K_{AA} are the intramode and K_{NA} the intermode coagulation coefficients, g^* is the number of molecules in the critical droplet and μ the molecular mass, R_{Cji} is the condensation rate of *i*-vapor on *j*-mode particles, and k_j is the deposition velocity due to diffusion.

Eqs. (1-5) were derived by transforming the space-derivatives of Vouitsis *et al.* (2005) into time-derivatives by means of the transformation ($u_{DE}d/dx$) = (d/dt), thus assuming a constant sample velocity u_{DE} along the flow path. The variable dilution ratio as time progresses is taken into account by expressing the volume change (1/*V*) *dV*/*dt* in terms of *DR*. The latter is assumed to vary linearly during the timespan of primary dilution, i.e.,

$DR(t) = ((DR_m - 1)/\tau_D)t + 1$, where DR_m is the DR at the FPS outlet and τ_D is the time in which primary dilution is completed (Table 1). Downstream of the FPS and upstream of the secondary dilution system, the *DR* remains constant and equal to DR_m. During dilution, the sample temperature is also assumed to vary following an adiabatic mixing, according to:

$$(T_{DE} - T_{DAT})/(T_{E0} - T_{DAT}) = 1/DR(t) \qquad (6)$$

where DE corresponds to diluted exhaust, *E0* corresponds to initial conditions (raw exhaust) and *DAT* to the dilution air temperature. After dilution, the sample temperature is considered to remain constant.

The concentration of the main species in the raw exhaust is calculated using a simplified combustion model (Vouitsis *et al.*, 2005). The nucleation rate in Eqs. (1), (2), (4) is taken to be proportional to the square of the sulphuric acid saturation ratio. Thus a kinetically limited nucleation is considered and the number of

molecules in the critical droplet is taken equal to two. The initial vapor concentration of sulphuric acid is calculated assuming a value for the fuel sulphur conversion fraction (FSCF). This was considered to vary between 8 and 20% wt. when no oxidation after-treatment is used in the exhaust line, and between 50 and 90% wt. when a DOC was fitted in the exhaust line. These values are selected as representative of what is known so far for sulphur to sulphuric acid conversion in a diesel engine (see Vouitsis *et al.,* 2005) but they can vary in reality with operation mode. Their effect is therefore discussed in the results section. As mentioned above, no sulphate contribution from the lube oil was taken into account, due to the relatively high fuel sulphur content.

Different alkanes were considered to condense on the newly-formed nuclei and on the pre-existing particles. The molecular concentration of the alkane *Cn* (N_{Cn}) in the raw exhaust gas is calculated using the formula:

$$N_{Cn} = f_{cd}[HC]\frac{MW_{C3}}{MW_{ex}}\frac{N_{AV}}{MW_{Cn}}\rho_{ex} \quad (7)$$

where [HC] is the hydrocarbon concentration (mol C_3/kmol exhaust) measured by a Flame Ionization Detector (FID), calibrated with propane and MW_{C3}, MW_{Cn}, MW_{ex}, are the molecular weights of propane, C_n-alkane, and exhaust respectively (kg/kmol), N_{AV}, the Avogadro number (1/mol), and ρ_{ex} the exhaust density (kg/m^3). The fraction of total organics potentially condensing on the particulate phase (f_{cd}) is assumed to range between 10 and 30%, consistent to a typical diesel exhaust hydrocarbon profile (Ntziachristos and Samaras, 2000). Alkane parameters necessary to calculate condensation were obtained directly from, or approximated with, literature data: the vapor pressure from Lemmon and Goodwin (2000) and Chickos and Hanshaw (2004), the partitioning coefficient from Liang *et al.* (1997), the surface tension from Queimada *et al*. (2001). In addition, the diffusion coefficient was calculated according to Bird *et al*. (1960):

$$\frac{pD_{Cn}}{\left(p^*_{Cn}p^*_{DE}\right)^{1/3}\left(T^*_{Cn}T^*_{DE}\right)^{5/12}\left(\frac{!}{M_{Cn}}+\frac{1}{M_{DE}}\right)^{1/2}} = \alpha\left(\frac{T}{\sqrt{T^*_{Cn}T^*_{DE}}}\right)^{b} \quad (8)$$

where the asterisk denotes a critical property. p is the pressure and α and b are constants for non-polar gas pairs (α = 2.745 x 10^{-4}, b = 1.823). The density was calculated according to Perry' s Chemical Engineering Handbook (Liley et al., 1997):

$$\frac{1}{\rho_{Cn}} = \left(\frac{R_{gas}T^*_{Cn}}{p^*_{Cn}}\right)Z^{\nu}_{RA} \quad (9)$$

where ρ_{Cn} is the density, R_{gas} is the gas-law constant, and Z^{ν}_{RA} is a parameter regressed from experimental data (ν is calculated as, $\nu = 1.0\left(1.0 - \mathrm{T}^r_{Cn}\right)^{2/7}$, where T^R_{Cn} is the reduced temperature of each alkane.

All other variables required for the modeling were obtained from measurements: temperatures were measured in the raw exhaust, after the first and the second stage of primary dilution and at the end of the sample aging chamber, while the mass concentration of AM particles was determined from gravimetric

measurements. Mass concentration of NM particles was calculated from the SMPS measurement. The calculation of AM number concentration needs an assumption for the initial mean AM diameter. This is another model parameter which is used to adjust the AM modeling results to the measurements as will be presented in the following section. Table 2 summarizes the initial conditions considered for the two engine loads tested.

RESULTS AND DISCUSSION

Effect of aging time on particles

Fig. 2(a) shows the size distributions recorded at ML for DR = 32 for the three sample ATs. The NM number concentration increases by a factor of 2.2 from short AT to medium AT and by a factor of 4.2 from short AT to long AT, whiles the mass concentration increases by a factor of 4.7 and 20.9, respectively. On the other hand, the AM practically remains constant, independently of the sample AT. We use this finding to adjust the modeling results for the AM by adjusting the accommodation coefficient and the initial mean AM diameter. Figs. 2(b) and 2(c) compare the modeling results for the number and mass concentration of NM particles respectively with the experimental data.

With respect to particle number concentration in the NM (Fig. 2(b)) the model predicts that this largely depends on the FSCF considered. No new particle nucleation may be predicted for FSCF below ~ 6.5% due to suppression by the large surface area concentration of AM particles. On an absolute scale, a FSCF value of

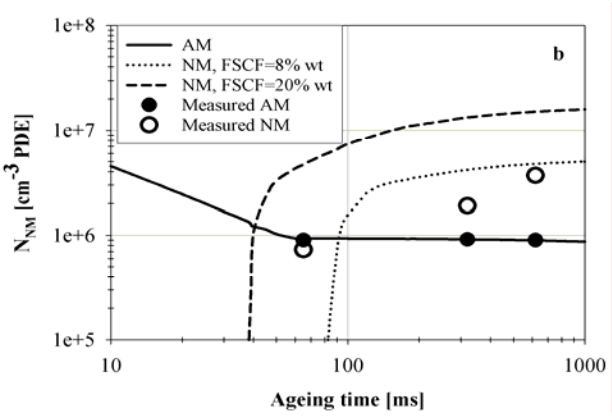

Fig. 2. (a) Effect of AT on particle size distribution for DR = 32:1 and medium load.

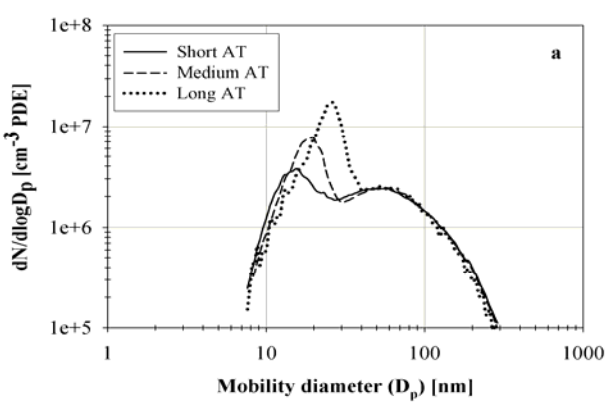

Fig. 2. (b) Evolution of number concentration as function of AT.

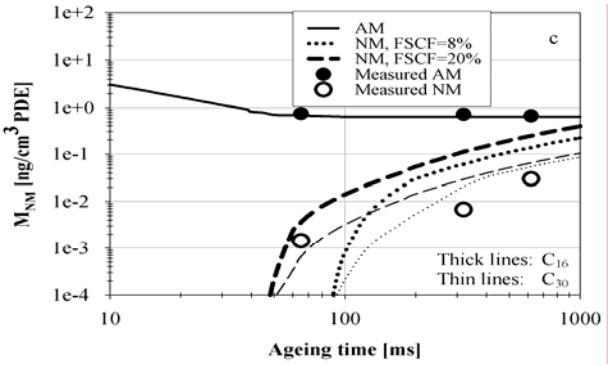

Fig. 2. (c) Evolution of mass concentration as function of AT for two different hydrocarbons considered. Dilution terminates at 55 ms and all concentrations refer to primary diluted exhaust (PDE).

8% seems to produce model results at the same level with the measurements, while a value of FSCF = 20% seems to overestimate final concentrations.

Fig. 2(c) shows the NM mass concentration evolution in the dilution chamber. In principle, all alkanes with carbon numbers larger than 14 would condense at the conditions tested (temperature always >30°C) but the maximum potential actually occurs for C_{16} molecules. Although the carbon number increase leads to both a reduction of the saturation vapor pressure and the activity coefficient, alkanes larger than C_{16} are more difficult to condense mainly due to their higher molar volume, which tends to increase the Kelvin effect for these species. In Fig. 2(c), the evolution of mass concentration of NM particles is shown for two alkanes (C_{16} and C_{30}) and a FSCF range of 8-20% wt. The behavior is similar to that of number: mass concentration increases rapidly due to the nucleation of SA and continues to increase until the end of the AT due to further condensation of both SA and hydrocarbons. The modeled absolute level and the trend of the mass concentration evolution in the NM are in some agreement with the experimental data, given the uncertainty in the selection of the FSCF value and the concentration and chemical type of the condensing species.

Effect of dilution ratio

Fig. 3(a) presents particle size distributions obtained at medium load, short AT and three different dilution ratios (10, 17, 32). In addition, size distributions at DR = 10 and 17 were also obtained downstream of the thermodenuder to provide soot mode size distributions without volatile particles. The soot mode concentration has been corrected for diffusional and thermodiffusional losses occurring in the thermodenuder. The comparison of size distributions obtained with and without the TD, shows that volatile particles seem to be formed at all dilution ratios; however, a clear distinction between NM and AM may not always be possible. In particular for DR = 10, when the volatile species concentration is maximum, volatile particles seem to grow beyond the typical NM range and the aerosol is dominated by these particles which give a monomodal shape to the size distribution. At higher dilution ratios, a bimodal distribution is obtained with the NM formed at DR = 17 being stronger than that formed at DR = 32. As several studies in the past have experimentally identified (e.g. Abdul-Khalek *et al.,* 1998; Mathis *et al.,* 2004b), the number and mass concentration of particles in the NM largely depend on the dilution ratio. It is therefore important to study whether these experimental results can be explained by modeling.

Fig. 3(b) compares the NM number concentration measured at different dilution ratios with the calculated results predicted, using again an FSCF range of 8-20% wt. The measured number concentration shown in the figure corresponds to the difference in the number concentrations without and with the TD in the sampling line. At DR = 32, where no measurement downstream of the TD is available, a lognormal distribution was fitted to the soot mode of this distribution and the number concentration of the NM was estimated

by subtracting this lognormal distribution from the measured bimodal distribution. The model predicts the effect of the dilution ratio on a relative scale, showing that the decrease of the DR leads to a higher number concentration, as the measured results also indicate. Although it fails to predict the number concentration measured for the low DR, it gives reasonable results for the higher DRs, especially when the higher FSCF value is assumed. However, a significant delay of the nucleation is predicted by the model compared to the experimental results. In principle, this means either that the supersaturation ratio increases faster locally in the dilution chamber, or that the cooling of the aerosol is faster than what is assumed by Eq. 6. The reasons for the faster nucleation observed need to be more thoroughly assessed, presumably by better estimating the flow development within the dilution chamber.

Fig. 3(c) shows the evolution of the particle mass in the nucleation mode, taking also into account the condensation of a C14-alkane on the pre-existing sulphuric acid particles. Mass concentrations show similar behavior to the number concentration. Again, the effect of dilution ratio on the nucleation mode mass is reasonably predicted with a delay of 50-200 ms, which should be attributed to the more rapid increase in the saturation ratio than what is assumed in the model. Without the addition of the alkane, it would not be possible for nuclei to increase in size, and the model would significantly understate the measured mass concentrations in Fig. 3(c). It is also obvious from Fig. 3 that low dilution ratios lead to a higher number and mass concentration of the nucleation mode. Hence, such sampling conditions should be preferred when nucleation mode particles are of interest.

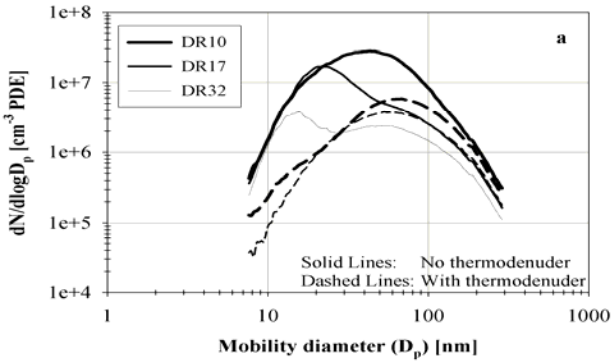

Fig. 3. (a) Size distributions at different dilution ratios and short AT, with and without the thermodenuder.

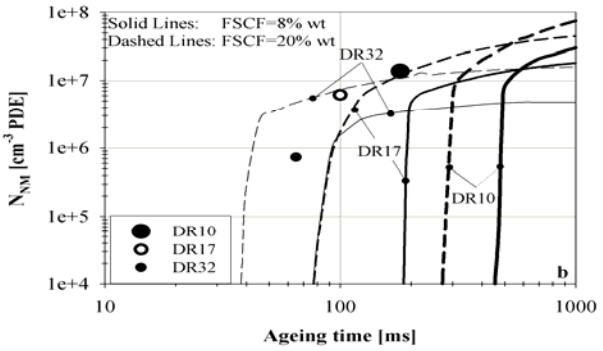

Fig. 3. (b) Evolution of NM number concentration as function of AT.

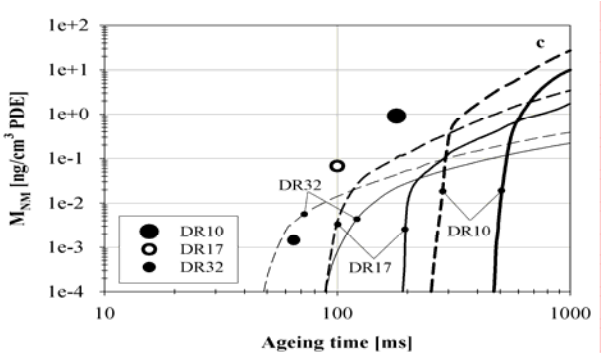

Fig. 3. (c) Evolution of the NM mass concentration as function of AT.

Effect of after-treatment devices

The previous sections showed that the model developed may satisfactorily predict the effect of sampling conditions on the observed size distributions of the nucleation mode particles. However, such a model would be useful not only to predict the effect of sampling conditions on number concentration, but also to estimate potential effects of engine modifications and after-treatment devices on nanoparticle emissions. In order to study the applicability of the model in such conditions, different after-treatment devices were installed in the vehicle exhaust line and a comparison between the measurements and the model predictions was performed.

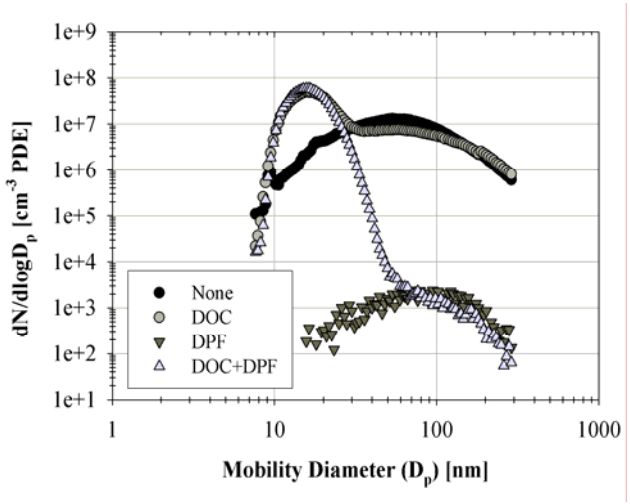

Fig. 4. Size distributions for different exhaust after-treatment configurations at short AT, high load and DR = 10.

Fig. 4 shows the mobility size distributions obtained at high engine load with different exhaust-line configurations and a DR of 10:1. The latter was shown to maximize the nucleation mode formation potential in the previous measurements (Fig. 3). When a DPF is fitted in the exhaust line, the accumulation mode number concentration decreases by four orders of magnitude, as a result of the high filtration efficiency of the DPF on solid particle emissions. However, the effect of DPF on the nucleation mode depends on the existence or not of a DOC in the exhaust line. Without the DOC, NM formation is suppressed in this operation condition, resulting in a lognormal particle size distribution, which remains four orders of magnitude lower than the engine-out concentration, regardless of particle size. Nevertheless, when the DOC is in place a distinct nucleation mode is formed, which is equal to size and number concentration to the NM formed without the DPF. Obviously, the oxidation activity of the catalyst in this case promotes the conversion of SO_2 to SO_3, which enables the formation of nanoparticles.

These four distinct aerosol distributions and exhaust gas compositions provide an ideal pattern to test and evaluate the main hypotheses of the model. The simulations are based on the measured exhaust gas conditions given in Table 2, regarding its temperature, hydrocarbon concentration, and mass and number concentrations of accumulation mode in the raw exhaust. It is also assumed that 10% of the total hydrocarbon concentration contributes to the particulate phase (Eq. 7). With regard to the FSCF, a range of values was again assumed to demonstrate the sensitivity of the model to this parameter. The range considered when a DOC was in place was 50-90%, compared to 8-20% when the catalyst was removed, due to the enhanced sulphur oxidation activity of the catalyst. This range is based on simple

Table 2. Temperature, hydrocarbon concentration and mass and number of particles in the accumulation mode at raw exhaust for different engine operation modes and after-treatment configurations.

Configuration	Load	T (°C)	[HC] (mol C_3/kmol exh)	M_{AM} (ng/cm^3)	$N_{AM} \times 10^{-7}$ (1/cm^3)	FSCF low-high (%)
Engine Out	Medium	265	0.077	21	3.00	8-20
Engine Out	High	392	0.110	54	7.75	8-20
DOC	High	380	0.033	54	7.75	50-90
DPF	High	409	0.110	0.001	1.40×10^{-4}	8-20
DOC+DPF	High	382	0.033	0.001	1.40×10^{-4}	50-90

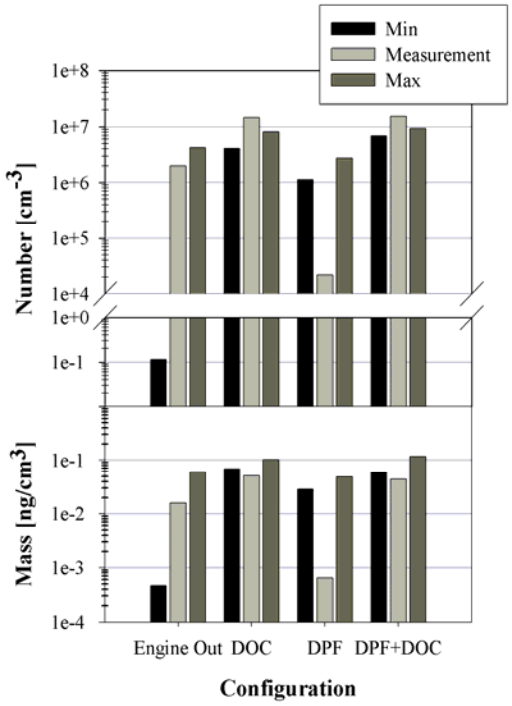

Fig. 5. Measured and modeled number (a) and mass (b) concentrations of nucleation mode at different exhaust pipe configurations and high engine load. The parameters for the minimum and maximum estimates are given on Table 2.

thermodynamic equilibrium considerations on the catalyst environment, but there are no experimental data to confirm them. By introducing these values to the model, Fig. 5 shows the comparison between model results and measurements, both for the number and the mass concentration of the NM. The min-max estimate corresponds to the range of FSCF values considered. For the engine-out condition, the model results are very sensitive to the FSCF value, with the calculated mass of NM ranging between two orders of magnitude, depending on the FSCF value assumed.

Therefore, the exact number and mass concentration calculated could have been reached by tuning the FSCF value considered. When a DPF is installed in the exhaust line (third group of bars), the model values exceed by far the measured number and mass concentration for both FSCF values considered. In this case, the model predicts a very high new particle formation, since no larger particle surface area is available to suppress the nucleation. The low measured values, however, show that in reality NM formation is much lower, which would mean that the actual sulphate concentration downstream of the DPF is lower than what the model considers. This may be, for example, an effect of sulphate adsorption on the soot layer in the DPF,

Table 3. Predicted composition of NM particles for different after-treatment configurations and modeling parameters.

Configuration	Sulphate (%)		Organics (%)	
	Low FSCF	High FSCF	Low FSCF	High FSCF
Engine Out	3.9	12.4	96.1	87.6
DOC	13.7	28.7	86.3	71.3
DPF	4.2	10.4	95.8	89.6
DOC+DPF	16.0	28.7	84.0	71.3

a process which has been shown to be favored when an engine works at high loads and a small specific surface is available (Durán *et al.*, 2003). On the contrary, the DOC installed in the exhaust line leads to particle number concentrations which are 50-70% higher than what the model predicts, even assuming 90% FSCF; while the total particle mass appears 30-50% lower than the simulated one. However, in both cases, given the uncertainties in the FSCF and hydrocarbon species profiles, the model adequately predicts the measured values.

Given the generally satisfactory comparison of the model and the measured results in number and mass concentration, it is of interest to show the chemical composition predicted for particles in the NM range, which is difficult to determine experimentally, due to their negligible mass. The calculated composition of the final NM mass is given in Table 3, which shows that organics are the dominant part in all cases and in engine-out condition in particular, in agreement with the results of Tobias *et al.* (2001) and Sakurai *et al.* (2003). This means that the sulphuric acid may be the primary source for the formation of stable nuclei. but contributes to a lesser extent to particle development by condensation.

CONCLUSIONS

The measurements showed that a distinct nucleation mode appears as fast as 60 ms after exhaust emission and continues to grow both in number and in mass for several hundreds of milliseconds in the sampling line. The nucleation mode number and mass concentration increase as the dilution ratio decreases, due to the higher concentration of volatile species in the diluted exhaust. An oxidation catalyst enhanced the nucleation mode number concentration while a particle filter decreased both the nucleation and the accumulation modes, except when combined with the oxidation catalyst, where a strong nucleation mode was observed.

Modeling results confirm the findings of our earlier work that an aerosol model consisting of a barrierless sulphuric acid nucleation mechanism and a hydrocarbon condensing mechanism may, in most cases, adequately predict the number and mass concentration of particles in the nucleation mode. When no exhaust after-treatment devices were installed in the exhaust line, the model provides reasonable estimations of particle number and mass concentration, assuming a fuel sulphur

conversion factor in the order of 8%. When a DOC is fitted in the exhaust line, higher fuel sulphur conversions (i.e. > 50%) are required to approach the measured number concentration.

The mass concentration of the nucleation mode is also satisfactorily predicted by the model, assuming that an alkane condenses on the pre-existing sulphuric acid particles. C_{16} alkanes seem to condense more easily due to the competing effects of the higher saturation ratio and the increase in the importance of the Kelvin effect as the hydrocarbon molecule increases. The condensation of a C_{14}-alkane (at a concentration equal to 30% of total hydrocarbons measured by FID) leads to a good prediction of the measured NM mass by the model. However, more detailed exhaust hydrocarbon speciation is required to predict the liquid mixture formed on the particle surface and to test the hypothesis that NM mass concentration can be estimated by using only alkanes as a surrogate of the exhaust organic species. More importantly, nanosized chemical analysis (e.g., Phuleria *et al.,* 2006) will show potential compositions of the NM particles.

ACKNOWLEDGMENTS

This work has been funded by the Greek Ministry of Education and by the European Union / European Social Fund (ESF). The authors wish to thank Dr. Barouch Giechaskel and Dr. Panayiotis Pistikopoulos for their support in the experimental work.

DISCLAIMER

Reference to any companies or specific commercial products does not constitute any advertisement or promotion of either.

REFERENCES

Abdul-Khalek, I., Kittelson, D.B. and Brear, F. (1998). Diesel Trap Performance: Particle Size Measurements and Trends. *SAE Technol. Paper* 982599.

Air Resources Board. (2003). *Proposed Amendments to the California Diesel Fuel Regulations. Staff Report: Initial Statement of Reasons. Appendix I: Diesel Engine Lubricating Oils*, Internet reference at http://www.arb.ca.gov/regact/ulsd2003/appi.pdf.

Bird, R. B., Stewart, W. E. and Lightfoot, E. N. (1960). *Transport Phenomena*, Wiley, New York, p. 505.

Burtscher, H. (2005). Physical Characterization of Particulate Emissions from Diesel Engines: A Review. *J. Aerosol Sci*. 36: 896-932.

Chickos, J.S. and Hanshaw, W. (2004). Vapor Pressures and Vaporization Enthalpies of the *n*-Alkanes from C21-C30 at T = 298.15 K by Correlation Gas Chromatography. *J. Chem. Eng. Data*. 49: 77-85.

CONCAWE. (2000). *Production of Ultra Low Sulphur Road Fuels (Including CO2, Air Quality and Greenhouse Effects*. Response to EU Commission "Call for evidence" on Ultra Low Sulphur (ULS) Fuels.

Durán, A., Carmona, M. and Ballesteros, R. (2003). Competitive Diesel Engine

Emissions of Sulphur and Nitrogen Species. *Chemosphere*. 52: 1819-1823.

Giechaskiel, B., Ntziachristos, L. and Samaras, Z. (2004). Calibration and Modelling of Ejector Dilutors for Automotive Exhaust Sampling, *Meas. Sci. Technol*. 15: 2199-2206.

Giechaskiel, B., Ntziachristos, L., Samaras, L., Scheer, V., Casati, R. and Vogt, R. (2005). Formation Potential of Vehicle Exhaust Nucleation Mode Particles on-Road and in the Laboratory. *Atmos. Environ*. 39: 3191-3198.

Gramotnev, D.K. and Gramotnev, G. (2005). Modelling of Aerosol Dispersion from a Busy Road in the Presence of Nanoparticle Fragmentation. *J. Appl. Meteorol*. 44: 888-899.

Hussein, T., Puustinen, A., Aalto, P.P., Mäkelä, J.M., Hämeri, K. and Kulmala, M. (2004). Urban Aerosol Number Size Distributions. *Atmos. Chem. Phys*. 4: 391–411.

Kittelson, D.B., Watts, W.F. Johnson., J.P. (2004). Nanoparticle Emissions on Minnesota Highways. *Atmos. Environ*. 38: 9–19.

Lemmon, E.W. and Goodwin, A.R.H. (2000). Critical Properties and Vapour Pressure Equation for Alkanes C_nH_{2n+2}: Normal Alkanes with $n \leq 36$ and Isomers for $n = 4$ through $n = 9$. J. *Phys. Chem. Ref. Data* 29: 1-39.

Liang, C., Pankow, J.F., Otum. J.R. and Seinfeld, J.H. (1997). Gas/Particle Partitioning of Semivolatile Organic Compounds to Model Inorganic, Organic, and Ambient Smog Aerosols. *Environ. Sci. Technol*. 31: 3086-3092.

Liley, P.E., Thomson, G. H., Friend, D.G., Daubert, T.E., Buck, E. (1997). In *Perry's Chemical Engineering Handbook*, R.H. Perry and D.W. Green (Eds.), McGraw–Hill, p. 2-358 and 2-372.

Mathis, U., Mohr, M. and Zenobi, R. (2004a). Effect of Organic Compounds on Nanoparticle Formation in Diluted Diesel Exhaust. *Atmos. Chem. Phys. Discus*. 4: 227–265.

Mathis, U., Ristimäki, J., Mohr, M., Keskinen, J., Ntziachristos, L., Samaras, Z. and Mikkanen, P. (2004b). Sampling Conditions for the Measurement of Nucleation Mode Particles in the Exhaust of Diesel Vehicle. *Aerosol Sci. Technol*. 38: 1149-1160.

Ntziachristos, L. and Samaras, Z. (2000). *COPERT III Computer Programme to Calculate Emissions from Road Transport*. European Environment Agency Report 49, Copenhagen, Denmark, p. 86.

Ntziachristos, L., Mamakos, A., Samaras, Z., Mathis, U., Mohr, M., Thompson, N., Stradling, R., Forti, L. and De Serves, C. (2004a). Overview of the European "Particulates" project on the Characterization of Exhaust Particulate Emissions from Road Vehicles: Results for Light-Duty Vehicles. *SAE Technol. Paper* 2004-01-1985.

Ntziachristos, L., Giechaskel, B., Pistikopoulos, P., Samaras, Z., Mathis, U., Mohr, M., Ristimäki, J., Keskinen, J., Mikkanen, P., Casati, R., Scheer, V. and Vogt, R. (2004b). Performance Evaluation of a Novel Sampling and Measurement System for Exhaust

Particle Characterization. *SAE Technol. Paper* 2004-01-1439.

Ntziachristos, L., Samaras, Z., Zervas, E. and Dorlhene, P. (2005a). Effects of a Catalysed and an Additized Particle Filter on the Emissions of a Passenger Car Operating on Low Sulphur Fuels. *Atmos. Environ*. 39: 4925-2936.

Ntziachristos L., Giechaskiel, B., Pistikopoulos. and Z. Samaras, Z. (2005b). Comparative Assessment of Two Different Sampling Systems for Particle Emission Type-Approval Measurements, *SAE Technol. Paper* 2005- 01-0198.

Phuleria, H.C., Geller, M.D., Fine, P.M. and Sioutas, C. (2006). Size-Resolved Emissions of Organic Tracers from Light-and Heavy-Duty Vehicles in a California Roadway Tunnel. *Environ. Sci. Technol*. 40: 4109-4118.

Queimada, A.J. Marucho, I.M, and Coutinho, J.A.P. (2001). Surface Tension of Pure Heavy n-Alkanes: A Corresponding States Approach. *Fluid Phase Equil.* 4639: 1-10

Rönkko, T., Virtanen , A., Vaaraslahti, K., Keskinen, J., Pirjola, L. and Lappi, M. (2006). Effect of Dilution Conditions and Driving Parameters on Nucleation Mode Particles in Diesel Exhaust: Laboratory and On-Road Study. *Atmos. Environ*. 40: 2893–2901.

.Sakurai, H., Tobias, H.J., Park, K., Zarling, D., Docherty, K.S., Kittelson, D.B., McMurry, P.H. and Ziemann, P.J. (2003). On-line Measurements of Diesel Nanoparticle Composition and Volatility. *Atmos. Environ*. 37: 1199–1210

Scheer, V., Kirchner, U., Casati, R., Vogt, R., Wehner, B., Philippin, P., Wiedensohler, A., Hock, N., Schneider, J., Weimer, S. And Stephan, B. (2005). Composition of Semi-volatile Particles from Diesel Exhaust. *SAE Technol. Paper* 2005-01-0197.

Tobias, H.J., Beving, D.E., Ziemann, P.J., Sakurai, H., Zuk, M., McMurry, P.H., Zarling, D., Waytulonis, R. and Kittelson, D.B. (2001). Chemical Analysis of Diesel Engine Nanoparticles Using a Nano-DMA/Thermal Desorption Particle Beam Mass Spectrometer. *Environ. Sci. Technol.* 35: 2233–2243.

Vaaraslahti, K., Virtanen, A., Ristimäki, J. and Keskinen, J. (2004). Nucleation Mode Formation in Heavy-Duty Diesel Exhaust with and without a Particulate Filter. *Environ. Sci. Technol*. 38: 4884-4890.

Vaaraslahti, K., Keskinen, J., Giechaskiel, B., Solla, A., Murtonen, T. and Vesala, H. (2005). Effect of Lubricant on the Formation of Heavy–Duty Diesel Exhaust Particles. *Environ. Sci. Technol.* 39: 8497–8504

Vogt, R., Scheer, V., Casati, R. and Bender, T. (2003). On–Road Measurement of Particle Emission in the Exhaust Plume of a Diesel Passenger Car. *Environ. Sci. Technol*. 37: 4070–4076.

Vouitsis, E., Ntziachristos, L. and Samaras, Z. (2005). Modelling of Diesel Exhaust Aerosol during Laboratory Sampling. *Atmos. Environ.* 39: 1335-1345.

Yu, F., Lanni, T. and Frank, B (2003). Measurements of Ion Concentration in Gasoline and Diesel Engine Exhaust. *Atmos. Environ*. 38: 1417-1423.

Zhang, K.M., Wexler, A.S. Zhu, Y.F.. Hinds, W.C. and Sioutas, C. (2004). Evolution of Particle Number Distribution near Roadways. Part II. The 'Road-to-Ambient' Process. *Atmos. Environ*. 38: 6655-6665.

Zhang, K.M., Wexler, A.S., Niemeier, D.A., Zhu, Y.F., Hinds, W.C. and Sioutas, C (2005). Evolution of Particle Number Distribution Near Roadways. Part III: Traffic Analysis and on-Road Size Resolved Particulate Emission Factors. *Atmos. Environ*. 39: 4155–4166.

Received for review, March 14, 2007
Accepted, September 4, 2007